THE JOURNAL OF BIOLOGICAL CHEMISTRY VOL. 287, NO. 14, pp. 11579–11591, March 30, 2012

Calcium/Calmodulin-dependent Protein Kinase Kinase 2 Regulates Macrophage-mediated Inflammatory Responses*[S]

Received for publication, December 20, 2011, and in revised form, February 11, 2012 Published, JBC Papers in Press, February 14, 2012, DOI 10.1074/jbc.M111.336032

Luigi Racioppi[‡§¶1], Pamela K. Noeldner[‡], Fumin Lin[‡], Stephanie Arvai[‡§], and Anthony R. Means[‡§¶]

From the Departments of [‡]Pharmacology and Cancer Biology and [§]Medicine, Duke University Medical Center, Duke University, Durham, North Carolina 27710 and the [¶]Department of Cellular and Molecular Biology and Pathology, University of Naples Federico II, 80131 Naples, Italy

Background: Calcium/calmodulin-dependent kinase kinase 2 (CaMKK2) acts, at least in part, in the hypothalamus to alter food intake and energy.
Results: CaMKK2 is expressed in macrophages and regulates the TLR4-mediated response to lipopolysaccharide.
Conclusion: CaMKK2 regulates macrophage-mediated inflammatory responses to nutrient excess and pathogens.
Significance: CaMKK2 is an attractive target for drugs that function to prevent inflammation associated with metabolic disorders and autoimmunity.

Calcium/calmodulin-dependent kinase kinase 2 (CaMKK2) plays a key role in regulating food intake and energy expenditure at least in part by its actions in hypothalamic neurons. Previously, we showed that loss of CaMKK2 protected mice from high-fat diet (HFD)-induced obesity and glucose intolerance. However, although pair feeding HFD to WT mice to match food consumption of CAMKK2-null mice slowed weight gain, it failed to protect from glucose intolerance. Here we show that relative to WT mice, HFD-fed CaMKK2-null mice are protected from inflammation in adipose and remain glucose-tolerant. Moreover, loss of CaMKK2 also protected mice from endotoxin shock and fulminant hepatitis. We explored the expression of CaMKK2 in immune cells and found it to be restricted to those of the monocyte/macrophage lineage. CaMKK2-null macrophages exhibited a remarkable deficiency to spread, phagocytose bacteria, and synthesize cytokines in response to the Toll-like receptor 4 (TLR4) agonist lipopolysaccharide (LPS). Mechanistically, loss of CaMKK2 uncoupled the TLR4 cascade from activation of protein tyrosine kinase 2 (PYK2; also known as PTK2B). Our findings uncover an important function for CaMKK2 in mediating mechanisms that control the amplitude of macrophage inflammatory responses to excess nutrients or pathogen derivatives.

Calcium functions as a second messenger to regulate a plethora of biological processes by forming a complex with calmodulin (CaM)[2] (1). Upon Ca^{2+} binding, CaM interacts with many targets, including three multifunctional CaM kinases (CaMKI, CaMKII, and CaMKIV). For full activation, CaMKI and CaMKIV require phosphorylation of an activation loop threonine by CaMKKα or CaMKKβ (also named 1 and 2, respectively). The requirement of two CaM kinases in the same signaling pathway is reminiscent of the mitogen-activated protein (MAP) kinase cascade and led to the concept of a CaM kinase cascade (2). Increasing evidence demonstrates that CaMKs control important functions in immune cells, and in turn, regulate the innate and adaptive immune responses (3–8). Finally, the AMP-dependent protein kinase has been identified as a third direct substrate of CaMKK2 (9–12).

We have identified a CaMKK2/AMP-dependent protein kinase pathway that functions to link Ca^{2+} signaling to energy expenditure and metabolic response to stress by regulating the production of the orexigenic hormone neuropeptide Y in the hypothalamus. Thus, genetic ablation of CaMKK2 protects mice from diet-induced obesity, insulin resistance, and glucose intolerance (13). Because obesity is associated with a chronic inflammatory response that, in turn, causes abnormalities in glucose metabolism, we reasoned that this phenotype might also occur if loss of CaMKK2 mitigates the innate immune response to overnutrition (14, 15). This prompted us to explore the role of CaMKK2 in mechanisms regulating the responsiveness of immune cells such as macrophages to pathogens and stressing agents. Indeed, in assessing CaMKK2 expression in immune cell types, we found that it was restricted to those of the monocyte/macrophage lineage.

Macrophages are phagocytes that play an essential role in clearing the body of debris, apoptotic cells, and pathogens (16). In lean subjects, macrophages display an attenuated inflammatory phenotype and protect adipose from metabolic stress. Contrariwise, in response to overnutrition, monocytes recruited to adipose develop into macrophages with a pro-inflammatory phenotype that plays a causative role in the glucose

* This work was supported, in whole or in part, by National Institutes of Health Grant GM033976 (to A. R. M.).
[S] This article contains supplemental Figs. 1–6.
[1] To whom correspondence should be addressed: Division of Cellular Therapy, Dept. of Medicine, Duke University Medical Center, 213 Research Dr., Box 3961 DUMC, 245 CARL Bldg., Durham, NC 27710. Tel.: 919-668-2971; Fax: 919-681-7060; E-mail: luigi.racioppi@duke.edu.
[2] The abbreviations used are: CaM, calmodulin; CaMK, CaM kinase; CaMKKα or -β, Ca^{2+}/calmodulin-dependent protein kinase; TLR, Toll-like receptor; GalN, D(+)-galactosamine hydrochloride; BM, bone marrow; BMDM, bone marrow-derived macrophages; HFD, high-fat diet; PYK2, protein tyrosine kinase 2; EGFP, enhanced green fluorescent protein; VAT, visceral white adipose tissue; C/EBP, CCAAT/enhancer-binding protein; Z, benzyloxycarbonyl; FMK, fluoromethyl ketone; ITAM, immune receptor tyrosine-based activation motif; pPYK2, phospho-PYK2; TRITC, tetramethylrhodamine isothiocyanate.

intolerance and metabolic syndrome associated with obesity (17). Because macrophages secrete a multitude of mediators that regulate all aspects of host defense, inflammation, and homeostasis, they play a critical role in the pathogenesis of sepsis and many other conditions characterized by an abnormal response to pathogens and stressing agents (18, 19). Therefore, we examined the role of CaMKK2 in the activation and function of macrophages

Here we report that loss of CaMKK2 attenuated the inflammatory response in adipose, and this helps to prevent the glucose intolerance induced by high-fat diet (HFD). Ablation of CaMKK2 also protected mice from endotoxin shock and fulminant hepatitis (18, 19) by markedly decreasing the responsiveness of macrophages to LPS. Finally, loss of CaMKK2 decreased accumulation of PYK2 in macrophages, which impaired the activation of p65 NFκB, ERK, Jun, and AKT. Collectively, our findings uncover an important function for CaMKK2 in regulating mechanisms that control the amplitude of the macrophage inflammatory response induced by nutrient excess or pathogens.

EXPERIMENTAL PROCEDURES

Mouse Strains

CaMKK2$^{-/-}$ mice have been described elsewhere (13). The targeting construct for deleting CaMKK1 was made using the triple lox vector series (20) with diphtheria toxin and TK-neomycin cassettes for selection. The long combination arm (EcoRI/SpeI fragment) and floxed segment (SpeI/NotI fragment) were obtained from a mouse (strain 129/SvEv) λ phage DNA library and cloned into the LoxL and LoxC vectors, respectively. The short arm was created by PCR using high-fidelity polymerase (AccuTaq, Sigma-Aldrich) and cloned into the AscI/EcoRI sites of the LoxR vector. The targeting construct was assembled from those three vectors and contained exons 2–8 of CaMKK1 flanked by loxP sites, a 6.6-kb long arm, and a 1-kb short arm for homologous recombination. The targeting construct was introduced into embryonic stem cells by electroporation, and targeted clones were identified by PCR and Southern analysis. Positive cells were transfected with Cre and screened for deletion of the floxed DNA. Cells with the deletion were used to create chimeric mice by blastocyst injection. Chimeric offspring were crossed with C57BL/6 mice, and pups were screened by PCR on genomic DNA isolated from tail cuts for CaMKK1-null and WT mice and backcrossed to C57BL/6 mice for several generations. Double KO mice were generated crossing CaMKK2$^{-/-}$ with CaMKK1$^{-/-}$ mice. Tg(Camkk2-EGFP)DF129Gsat mice were provided by the Mutant Mouse Regional Resource Centers (MMRRCC). This transgenic strain contains the coding sequence for enhanced green fluorescent protein (EGFP), followed by a polyadenylation signal, inserted into the mouse genomic bacterial artificial chromosome RP23-31J24 at the ATG transcription initiation codon of the calcium/calmodulin-dependent protein kinase kinase 2 β (*Camkk2*) gene so that expression of the reporter mRNA/protein is driven by the regulatory sequences of the mouse gene (21).

Pair Feeding on High-fat Diet

Fourteen WT and *CaMKK2*-null mice about 3 months of age were selected for this study and housed in individual cages. Food intake and body weight were monitored daily. CaMKK2-null mice had free access to the high-fat diet or low-fat diet containing 58 and 10.5% kcal from fat, respectively (D12330 and D12328, Research Diets, New Brunswick, NC). WT mice would eat more food if it was provided *ad libitum*, and so they received the average amount of the food consumed by the CaMKK2-null mice. All mice had free access to water. The food was provided to mice every day at 5 p.m., 1 h before the dark cycle began. Pair feeding was carried out for 30 weeks; dual energy x-ray absorptiometry scan, glucose tolerance test, and insulin tolerance test were performed at the end. To avoid possible effects of starvation, mice had free access to high-fat diet for 2 days prior to euthanization. Epididymal fat pads from WT and CaMKK2-null mice of comparable body weight and adiposity were isolated for RNA extraction.

Dual Energy X-ray Absorptiometry

Mice were anesthetized (ketamine, 100 mg/kg; xylazine, 10 mg/kg) and scanned four times (with no repositioning between scans) using a Lunar PIXImus II densitometer (software version 2.0; GE Lunar Corp.). Measurements were typically performed between 8:00 a.m. and 11:30 a.m. Anesthetized mice were placed on the imaging-positioning tray in a prostrate fashion with the front and back legs extended away from the body. Heads were excluded from all analyses by placing an exclusion region of interest over the head. Thus, all body composition data exclude the head.

Glucose Tolerance Test

Glucose tolerance assays were performed on mice that were fasted overnight (>12 h). At 9:00 a.m., mice were measured for baseline glucose by collecting a small drop of blood from the tail vein for analysis using a handheld Bayer Ascensia Contour glucometer. After the baseline glucose values were established, each mouse was weighed and given an intraperitoneal injection of 2 mg of glucose/g of body weight (D14-212, Fisher Scientific). Blood glucose was quantified as a function of time until glucose levels returned to near baseline values.

Analysis of Adipose Macrophages

Epididymal fat pads isolated from freshly sacrificed WT and CaMKK2-null mice were minced and digested with collagenase P (11249002001; Roche Applied Science) dissolved in DMEM with 5% fat-free BSA at a concentration of 1 mg/ml. Tissues were incubated at 37 °C for 45 min and filtered through a sterile 230-μm stainless steel tissue sieve (1985-00069; Bellco Glass, Vineland, NJ). After centrifugation at 500 × *g* for 10 min, the pelleted cells were stained with lineage-specific antibodies and analyzed by flow cytometry. Mouse BD Fc Block (BD Pharmingen) was employed to block unwanted binding of antibodies. Dead cells were excluded by analysis of cell size and staining with 7-amino actinomycin (BD Pharmingen). Appropriate isotype controls were used to evaluate nonspecific staining (BD Pharmingen). 7-Amino actinomycin-negative macrophages

were identified by co-expression of F4/80 and I-A (MHC class II). Analyses were performed using a FACScan (BD Biosciences) and FlowJo Software (TreeStar, Ashland, OR).

RNA Isolation and Real-time PCR

Total RNA from visceral adipose tissue (VAT) and macrophages were isolated using TRIzol (Invitrogen) or the QIAquick PCR purification kit (Qiagen, Valencia, CA), respectively. Single-stranded cDNA was synthesized using SuperScript II reverse transcriptase (Invitrogen) according to the manufacturer's directions. Real-time PCR was carried out using an iCycler (Bio-Rad) with the IQ SYBR Green supermix (Bio-Rad). After deriving the relative amount of each transcript from a standard curve, transcript levels were normalized to 18 S ribosomal RNA. PCR primers for cytokines, chemokines, transcription factors, PYK2, and housekeeping genes were from Qiagen (RT^2 quantitative PCR primer assays, SAbiosciences).

Endotoxin Shock and Fulminant Hepatitis

Endotoxemia was induced by intraperitoneal injection of lipopolysaccharide (LPS, *Escherichia coli 055:B5*; Sigma-Aldrich) alone or in combination with D(+)-galactosamine hydrochloride (GalN, Sigma-Aldrich), dissolved in 0.2 ml of PBS, at the doses indicated in the figure legends. Livers were collected at the time points indicated in the figure legends, fixed in formalin, and embedded in paraffin. Apoptotic cells were detected using a TUNEL assay kit (Promega, Fitchburg, WI) according to the manufacturer's instructions. Nuclei were identified by DAPI staining (blue). Macrophages were detected by using F4/80, rat anti-mouse antibody (Invitrogen), and ABC VECTASTAIN kit, according to the manufacturer's instructions (Vector Laboratories Inc., Burlingame, CA). The number of TUNEL+ and DAPI+ cells (green and blue, respectively) and F480+ cells was quantified by using Image-based Tool for Counting Nuclei (ITCN) plug-in for the ImageJ software (National Institutes of Health, Bethesda, MD).

Generation of Cells

Bone Marrow-derived Macrophages (BMDM)—Hind limb bones were removed from mice and crushed in a mortar with 5 ml of Hanks' balanced salt solution (Mediatech, Manassas, VA), plus 2% FBS (Gemini Bio-Products, West Sacramento, CA) supplemented with 20 mM HEPES. Bone marrow (BM) cell suspensions were passed through a 70-μm strainer (BD Falcon) and stratified on Lympholyte (Cedarlane, Burlington, NC). The low-density fraction containing BM nucleated cells was collected, and the concentration was adjusted to 2×10^6 cells/ml in complete medium (10% fetal calf serum DMEM, high glucose, supplemented with glutamine, pyruvate, and HEPES, no phenol red) containing 30% L929-conditioned medium (bone marrow macrophage medium). Then, BM cells were cultured 6 days in Corning® Costar® Ultra-Low attachment multiwell plates (Sigma). To establish the purity of BMDM, cells were double-stained with anti-CD11b and anti-F4/80 antibodies. Based on this analysis, more than 95% of cells co-expressed these markers, which is typical for macrophages.

Peritoneal Macrophages—Peritoneal cells were collected according to the protocol reported elsewhere (22). Peritoneal cell suspensions were adjusted to the concentration of 2×10^6 cells/ml in complete medium and left to adhere to a cell culture dish for 2 h at 37 °C, 5% CO_2. To isolate peritoneal macrophages (adherent), nonadherent cells were removed by gentle agitation of dishes using complete medium.

Stimulation of Macrophages

BMDM were collected from BMM medium and cultured at a density of 2×10^4 and 5×10^4 cells/well on 12- or 6-well plates, respectively, in complete medium. After a 4-h cultivation at 37 °C, cells were stimulated with LPS at the concentrations reported in the figure legends. At the indicated times, supernatant fluids were collected for cytokine detection, and cells were lysed in the appropriate buffers for protein and RNA analyses. The protease inhibitor MG132 (Sigma) was dissolved in sterile dimethyl sulfoxide (DMSO; Sigma) at a concentration of 42 mM. Solutions were kept frozen in aliquots at −80 °C and used at a final concentration of 10 μM. Ammonium chloride (Sigma) was used at a final concentration of 50 mM.

Immunocytochemistry

BMDM were collected from BMM medium and cultured in complete medium at a density of 0.5×10^4 on glass coverslips for 4 h before being stimulated with LPS at the concentrations and times reported in the figure legends. To analyze morphological changes, cells were fixed for 10 min in 1% paraformaldehyde, PBS and stained with phalloidin-TRITC for 15 min. Glass coverslips were mounted in hard-set mounting medium (VECTASHIELD, Vector Laboratories). Images were acquired using a Zeiss AxioVert 200M widefield microscope connected to an AxioCam MRm camera. Images were taken using a 20× objective and post-processed by contrast and brightness enhancement within the AxioVision 4.8.2 software (Carl Zeiss MicroImaging). Images were quantified by using the ITCN plug-in for the ImageJ software. To this end, images were first converted in 8-bit mode, the threshold was adjusted to clearly identify individual cells, and then macrophage borders were tracked to measure the area of each cell. The mean ± S.D. of area was calculated from 20 independent fields.

Immunoblot

BMDM were washed three times with 2 ml of ice-cold PBS and lysed with 0.15 ml of M-PER mammalian protein extraction reagent with Halt protease and phosphatase inhibitor (Thermo Scientific). Equal amounts of protein sample/lane were denatured and resolved by SDS-PAGE. Proteins were transferred to Immobilon-FL membrane (Millipore, Billerica, MA), and quantitative Western blotting was performed using the Odyssey infrared Western blotting detection system (LI-COR Biosciences, Lincoln, NE). Primary antibodies used were anti-CaMKK (BD Biosciences); anti-actin (Sigma-Aldrich); anti-phospho-c-Jun and anti-α-tubulin (Santa Cruz Biotechnology, inc.); and anti-PYK2, anti-phospho-PYK2 (Tyr^{402}), anti-c-Jun, anti-phospho-ERK1/2 (Thr^{202}/Tyr 204), anti-ERK, anti-pNFκB p65 (Ser^{536}), anti-pNFκB p65, anti-phospho-AKT (Thr^{308}), anti-AKT, anti-phopspho-p38 (Thr^{180}, Tyr^{182}), and

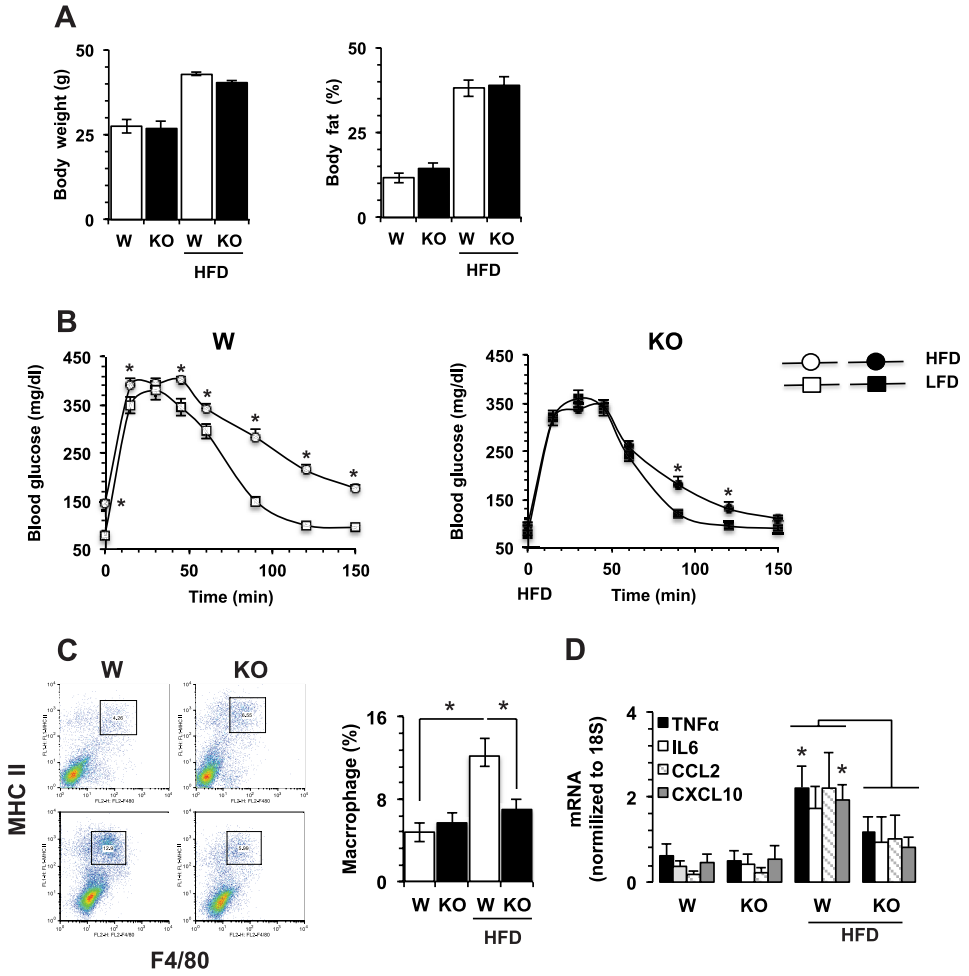

FIGURE 1. **CaMKK2$^{-/-}$ mice are resistant to high-fat diet-induced glucose intolerance and inflammation in adipose.** WT and CaMKK2$^{-/-}$ mice (*W* and *KO*, respectively) were housed five per cage and pair-fed an HFD (D12330) from Research Diets for 36 weeks. *A*, WT and KO mice of comparable body weight and fat percentage (measured by dual energy x-ray absorptiometry and dual energy x-ray absorptiometry scans) at weaning age and after 36 weeks of HFD (n = 10 each group). *B*, on the HFD, KO mice remain glucose-tolerant. *LFD*, low-fat diet. *C*, WT and KO mice show comparable accumulation of macrophages in VAT at the age of weaning (upper dot plot panels and left bar graphs). KO mice are protected from macrophage accumulation in VAT induced by 36 weeks HFD (lower dot plot panels and right bar graphs). *D*, WT and KO mice show comparable accumulation of cytokine and chemokine mRNAs at weaning. On the HFD, WT mice show significantly higher levels of TNFα and CXCL10 as compared with KO mice. mRNAs were quantified by real-time PCR. $n = 4$; *, $p < 0.01$.

anti-p38 from Cell Signaling (Danvers, MA). Secondary antibodies used were anti-mouse IgG Alexa Fluor 680 (Invitrogen) and anti-rabbit IgG IRDye800-conjugated antibody (Rockland Immunochemicals, Gilbertsville, PA).

Cytokine Detection

Cytokines in BMDM supernatant fluids were measured by BioLegend ELISA MAX kits (BioLegend, San Diego, CA), according to the manufacturer's instructions. Cytokines and chemokines in mouse sera were analyzed by RodentMAP® version 2.0 (Myriad RBM, Austin, TX).

Statistical Analysis

Statistical analysis was performed with GraphPad Prism software (GraphPad) by using Student's *t* test. All survival curves were compared by the log-rank test. Statistical analyses in multiple comparison groups (see Figs. 1, *C* and *D*, 5, *A* and *B*, and 6, *B–E*) were performed by using one-way analysis of variance test.

RESULTS

Genetic Ablation of CaMKK2 Protects Mice from Effects of High-fat Diet—We previously reported that CaMKK2 plays a key role in the pathway by which ghrelin signals to AMP-dependent protein kinase to regulate expression of the orexigenic neuropeptide Y peptide in hypothalamic neurons, protecting mice from diet-induced obesity, insulin resistance, and glucose intolerance (13). Because obesity is associated with a chronic inflammatory response, we also compared the effects induced by HFD on accumulation of macrophages and CD4$^+$ FOXP3$^+$ regulatory T cells (Treg) in spleen. As expected, HFD induced a significant increase of macrophages in WT mice, and this was associated with a parallel decrease in the percentage of regulatory T cells (supplemental Fig. 1). Because this phenotype might occur because CaMKK2 KO mice have reduced diet-induced obesity, thus accounting partially or completely for the attenuated inflammatory response (14, 15), we selected WT and CaMKK2$^{-/-}$ mice of comparable body weight and fat accumulation at weaning, pair-fed them an HFD for 36 weeks,

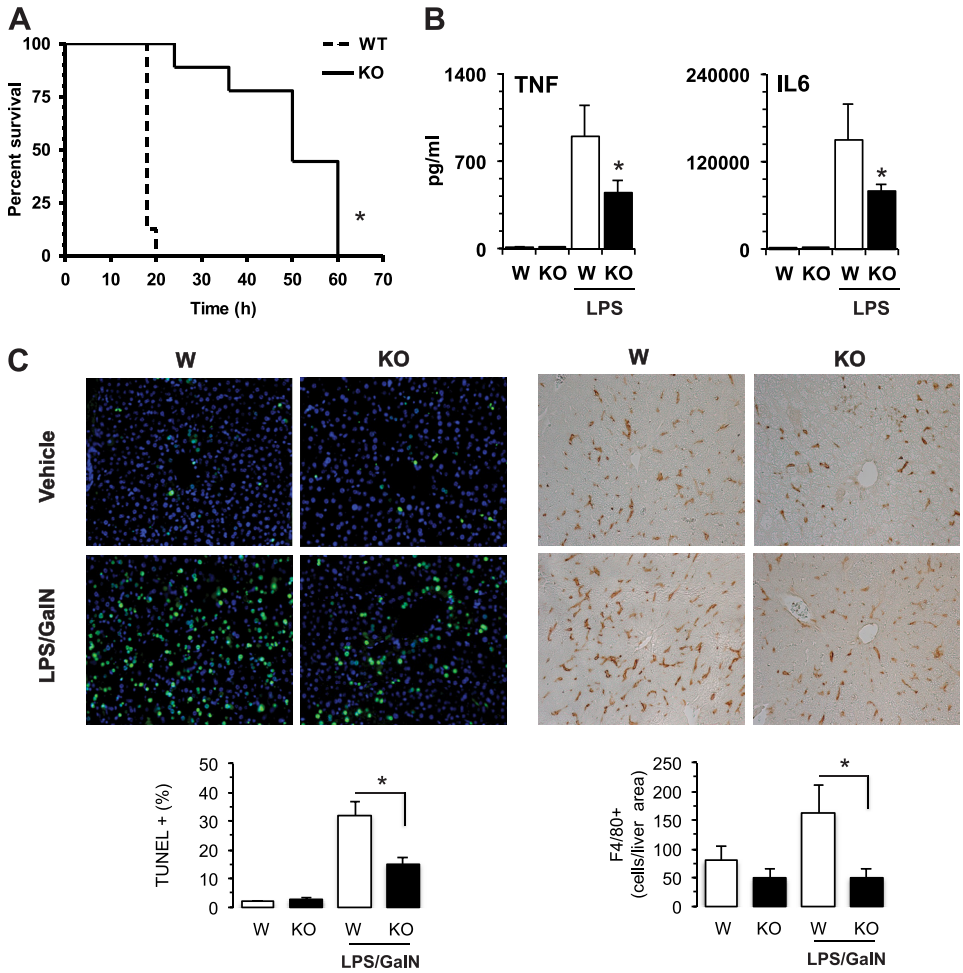

FIGURE 2. **Loss of CaMKK2 protects mice from shock and hepatitis induced by lipopolysaccharide.** Wild type (*W*) and CaMKK2-null mice (KO) were injected intraperitoneally with LPS (15 mg/kg of body weight). *A*, survival curves ($n = 10$ mice, each genotype). *B*, sera were collected, and cytokines were evaluated at 3 h. *C*, loss of CaMMK2 protects from fulminant hepatitis. WT and KO mice were injected intraperitoneally with low doses of LPS (1.5 mg/kg of body weight) plus GalN (700 μg/kg of body weight) or vehicle. After 6 h, livers were collected and fixed in formalin for 18 h. *Upper left*, detection of apoptotic cells by TUNEL assay. *Green* and *blue* identify apoptotic cells and nuclei (TUNEL+ and DAPI+, respectively). *Upper right*, representative staining of macrophages using F4/80 antibody. *Lower*, histograms show quantification of the percentage of apoptotic cells (*green*) on total cells (*blue*) and the number of F4/80$^+$ cells detected in each field of liver histological section (*left* and *right*, respectively). Mean ± S.D. represents 20 independent histological sections from four mice of each genotype. *, $p < 0.001$.

and then again selected WT and CaMKK2 KO mice of comparable body weight for further study (Fig. 1*A*). First, we evaluated these mice for glucose tolerance and macrophage accumulation in VAT. As expected, WT mice developed glucose intolerance as a function of time (Fig. 1*B*), as well as a marked increase of activated macrophages in adipose (Fig. 1*C*). HFD feeding also induced a significant accumulation of TNFα and CXCL10 mRNA in VAT (Fig. 1*D*). Although CaMKK2 KO mice became obese on the HFD, they remained tolerant to glucose (Fig. 1, *A* and *B*). Moreover, glucose tolerance curves between CaMKK2$^{-/-}$ mice fed with high-fat and low-fat diets were largely overlapping (Fig. 1*B*). Finally, CaMKK2$^{-/-}$ mice fed with HFD did not accumulate activated macrophages in adipose (Fig. 1*C*). Moreover, we found significantly lower levels of TNFα and CXCL10 mRNA in VAT of HFD-fed CaMKK2 KO mice as compared with WT (Fig. 1*D*). Thus, genetic ablation of CaMKK2 completely dissociated the effects of HFD on body weight and fat accumulation from those on the inflammatory response and glucose tolerance. Overall, these findings support the hypothesis that in addition to its effects on food intake, CaMKK2 also regulates inflammation in VAT in response to high-fat feeding.

Genetic Ablation of CaMKK2 Protects Mice from Shock and Fulminant Hepatitis Induced by LPS—Based on the attenuated inflammatory response of CaMKK2-null mice to overnutrition, we investigated the role for CaMKK2 in two models of inflammation triggered by systemic exposure to LPS, endotoxin shock and fulminant hepatitis. Indeed, CaMKK2-null mice showed markedly prolonged survival to LPS (15 mg/kg of body weight, Fig. 2*A*). This was associated with a significantly decreased accumulation of TNFα and IL6 in serum collected 3 h after LPS injection (Fig. 2*B*). A more extensive analysis confirmed these data, revealing a marked decrease in the ability of CaMKK2 KO mice to accumulate multiple cytokines and chemokines 10 h after LPS administration (supplemental Fig. 2). Additionally, we evaluated the role of CaMKK2 in a model of fulminant hepatitis, which is characterized by a severe inflammatory response in liver that is induced by lower doses of LPS when administered in combination with the transcription inhibitor GalN. We found a profoundly decreased number of apoptotic cells in the

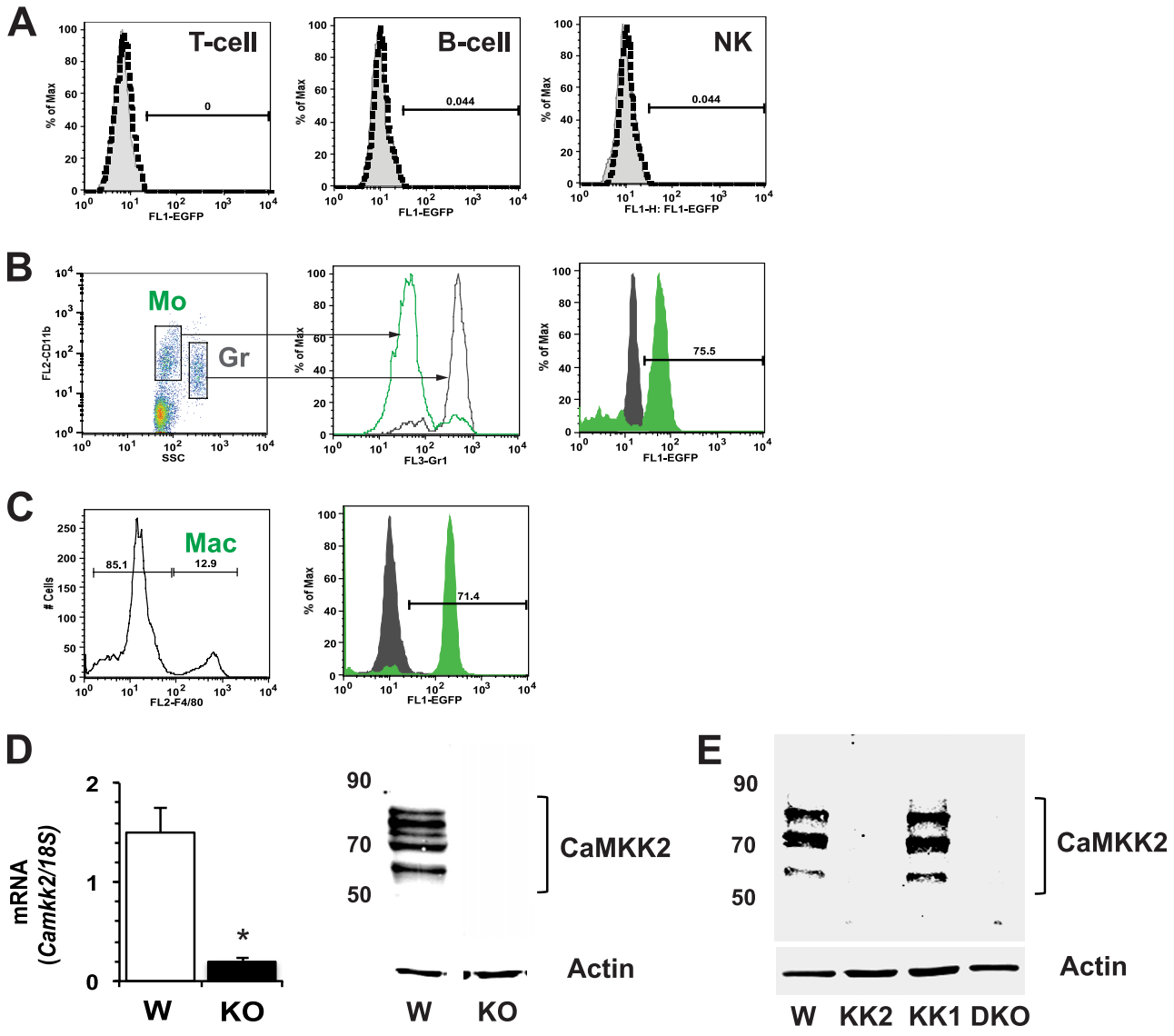

FIGURE 3. **CaMKK2 expression in immune cells.** EGFP expression in immune cells isolated from blood and peritoneum of Tg(Camkk2-EGFP) mice was measured. *A*, EGFP expression in $CD3^+$, $CD19^+$, and $CD3^-/NK1.1^+$ blood cells (T, B, and natural killer (*NK*), respectively). *B*, gating strategy to identify EGFP+ blood myeloid cells (*left* and *middle panels*). *Right*, EGFP expression in monocytes (*Mo*, small $CD11b^+/Gr1^-$ cells, *solid green profile*) and granulocytes (*Gr*, large $CD11b^+/Gr1^+$ cells, *solid black profile*). *C*, cells isolated from peritoneal lavage of Camkk2-EGFP mice were stained for the macrophage marker F4/80 (*Mac*, *left*). *Right*, EGFP expression in $F4/80^-$ and $F4/80^+$ cells (*black* and *green profiles*, respectively). *D*, CaMKK2 expression in BMDM generated from wild type and $CaMKK2^{-/-}$ mice (*W* and *KO*, respectively). *Left*, CaMKK2 mRNA expression. *Right*, CaMKK2 expression was evaluated by immunoblot with a pan-CaMKK antibody. *E*, CaMKK2 expression in peritoneal macrophages isolated from WT, $CaMKK2^{-/-}$, $CaMKK1^{-/-}$, and $CaMKK2^{-/-}$ $CaMKK1^{-/-}$ double KO mice (*W*, *KK2*, *KK1*, and *DKO*). CaMKK2 expression was evaluated by immunoblot with a pan-CaMKK antibody. *, $p < 0.001$.

liver of CaMKK2 KO mice exposed to LPS/GalN as compared with WT mice (Fig. 2*C*, *left*). Of note, many fewer infiltrating macrophages accumulated in the liver of $CaMKK2^{-/-}$ mice in response to LPS/GalN (Fig. 2*C*, *right*). Therefore, the loss of CaMKK2 results in an attenuated inflammatory response induced either by chronic exposure to excess nutrients or by an acute challenge with LPS.

CaMKK2 Is Selectively Expressed in Macrophages—CaMKK2 is expressed at high levels in brain, but its expression in other cells and tissues is considerably restricted (2). To examine whether cells in the periphery could be involved in the protection of CaMKK2-null mice from metabolic stress induced by overnutrition, we evaluated liver, adipose, and spleen for the presence of CaMKK2 and could detect the mRNA but not protein in each tissue (data not shown). This suggested that rare cell types common to all three tissues might express CaMKK2. Because such cells include lymphocytes and macrophages, we employed bacterial artificial chromosome transgenic mice expressing the CaMKK2 promoter-specific fluorescent reporter protein (*Camkk2*-EGFP) to examine the activity of *Camkk2* promoter in immune cells (21). To this end, we collected peripheral blood, spleen, and peritoneal cells from *Camkk2*-EGFP mice and stained cells with phycoerythrin-conjugated lineage-specific antibodies. EGFP protein was undetectable in T, B, and natural killer cells from blood, spleen, and peritoneal lavage as well as in circulating granulocytes, as we recently reported (23) (Fig. 3*A*). Contrariwise, we found CaMKK2 expressed in circulating monocytes and in peritoneal

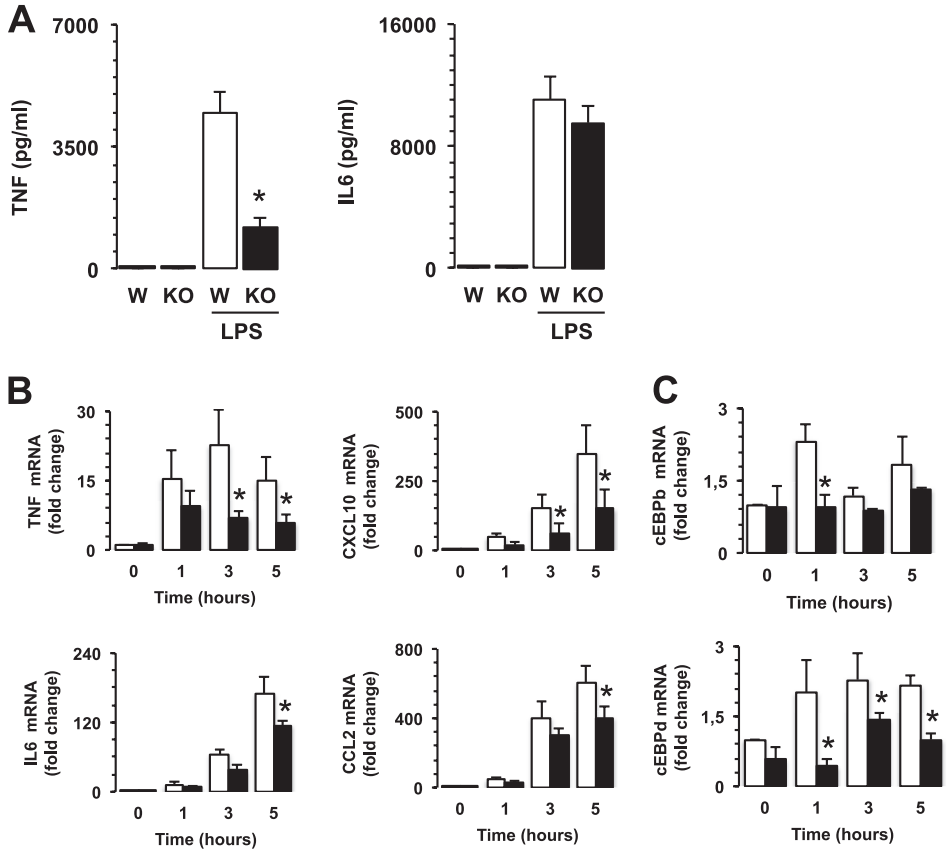

FIGURE 4. **Loss of CaMKK2 impairs response of bone marrow-derived macrophages to bacterial lipopolysaccharide.** BMDM were generated from WT (*W*) and CaMKK2$^{-/-}$ (*KO*) cells and exposed to LPS (100 ng/ml). *A*, cytokines in 24-h supernatant fluids. *B* and *C*, cytokine, chemokine, and transcription factor mRNAs detected in 1-, 3-, and 5-h LPS-stimulated WT and KO BMDM. *, $p < 0.001$.

cells expressing the macrophage marker F4/80 (Fig. 3, *B* and *C*). We conclude that in basal conditions, the activity of *Camkk2* promoter is restricted to the monocyte/macrophage lineage. To provide more direct evidence for this hypothesis, we generated macrophages from WT and CaMKK2-null bone marrow (BMDM) and identified CaMKK2 mRNA (Fig. 3*D*). Moreover, by using a pan-CaMKK-specific antibody, we clearly detected three major specific bands only in cell lysates obtained from WT macrophages (Fig. 3*D*). Although these data are compatible with the expression of the multiple isoforms of CaMKK2 in macrophages, we could not exclude the possibility that the pan-CaMKK2 antibody we used for the immunoblot also detected CaMKK1. To definitively exclude this possibility, we isolated peritoneal macrophages from WT, CaMKK2 KO, CaMKK1 KO, and CaMKK2/CaMKK1-double KO mice and clearly found the pan-CaMKK antibody to recognize specific bands corresponding to CaMKK2 only in WT and CaMKK1 KO macrophages (Fig. 3*E*). Thus, these data demonstrate that among immune cell types, expression of CaMKK2 is restricted to cells of the monocyte/macrophage lineage.

CaMKK2 Is Required for LPS-induced Cytokine and Chemokine Synthesis—To define the functions of CaMKK2 in macrophages, we compared the responsiveness of WT and CaMKK2-null BMDM to LPS. Although the absence of CaMKK2 did not significantly interfere with secretion of IL6, decreased TNFα was detected in the supernatant fluids of CaMKK2-null BMDM as compared with WT (Fig. 4*A*). We also examined the profile of mRNAs accumulated in WT and CaMKK2 KO macrophages exposed to LPS. Similar to our observation in VAT (Fig. 1*D*), we found a small decrease in IL6 and CCL2 mRNA only at later time points; however, the loss of CaMKK2 significantly impaired accumulation of TNFα and CXCL10 (Fig. 4*B*). Loss of CaMKK2 also impaired accumulation of other cytokine mRNAs including IL12a, IL12b, IL15, and IL10 (supplemental Fig. 3*A*). Finally, CaMKK2-null macrophages also accumulated significantly lower levels of several mRNAs encoding inducible inflammatory chemokines required for the recruitment of monocytes and effector T cells into inflamed tissues (24, 25), such as CCL3, CCL4, CCL5, and CCL7, as compared with WT (supplemental Fig. 3*B*). In contrast to that observed in serum (supplemental Fig. 2), LPS-stimulated CaMKK2$^{-/-}$ BMDM accumulated less CCL2 mRNA as compared with WT. In addition to macrophages, other cell types such as neutrophils can sense and respond to LPS (26). However, as shown in Fig. 3*A* and previously reported (23), neutrophils do not express CaMKK2. Thus, genetic ablation of this kinase would not impair the ability of neutrophils to release CCL2 in response to LPS. This may help explain the apparent discrepancy in the levels of CCL2 accumulating in serum *versus* isolated macrophages.

CCAAT/enhancer-binding protein (C/EBP) α, β, and δ are members of a family of basic region-leucine zipper (bZIP) transcription factors that are expressed in macrophages and regulate the expression of cytokine and chemokine genes in

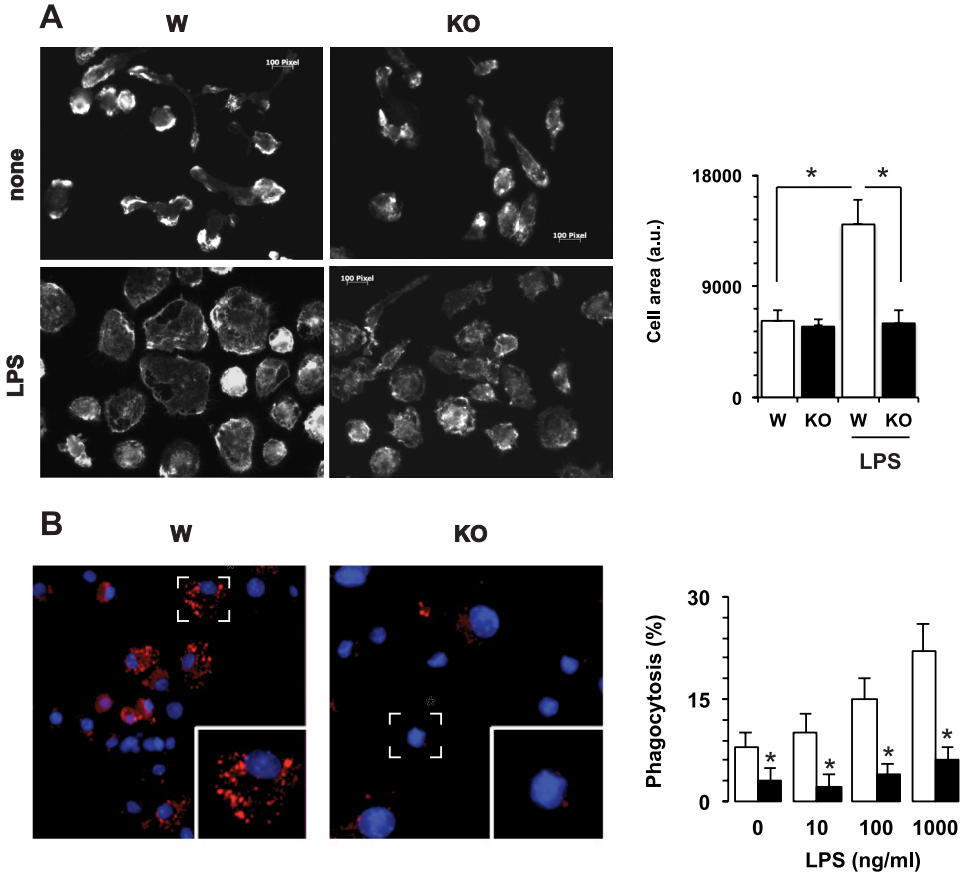

FIGURE 5. **Loss of CaMKK2 impairs response of bone marrow-derived macrophages to bacterial lipopolysaccharide.** *A*, effects of CaMKK2 ablation on macrophage spreading. *Left*, BMDM were cultured for 18 h in absence (none) or in the presence of LPS (100 ng/ml), fixed, permeabilized, and stained with phalloidin. The bar graph shows the average macrophage area calculated from 20 independent fields (*right*). *a.u.*, arbitrary units. *B*, BMDM from Wild type (*W*) and CaMKK2$^{-/-}$ (*KO*) were cultured in the presence or absence of LPS. After a 24-h incubation, cells were exposed for 2 h to pHrodo-conjugated *E. coli*. *Left panels* show the presence of pHrodo-*E. coli* in phagosomes (*red*). *Right panel*, BMDM were cultured in 96-well plates in the presence or absence of LPS (100 ng/ml). After 24 h, cells were incubated for 2 h with pHrodo-*E. coli*. Then, phagocytosis was quantified by luminometer and expressed as the percentage of maximal fluorescence measured in control samples exposed to an acidic pH. *Open* and *black bars* refer to WT and KO macrophages, respectively. *, $p < 0.001$.

response to LPS (27). To explore the effects of CaMKK2 ablation on these critical transcription factors, we evaluated c/EBP mRNA levels in quiescent and LPS-stimulated macrophages. c/EBPα, c/EBPβ, and c/EBPδ accumulated with different kinetics in quiescent and LPS-stimulated WT BMDM. We found the expression of c/EBPα mRNA to be high in quiescent WT BMDM but that it progressively declined after exposure to LPS (supplemental Fig. 3*A*). Kinetics of c/EBPβ mRNA accumulation showed a rapid and transient increase, which peaked 1 h after the LPS stimulus and then rapidly declined at later time points (Fig. 4*C*). LPS also induced a rapid increase in c/EBPδ mRNAs, but this mRNA remained stable over time (Fig. 4*C*). Quiescent CaMKK2-null macrophages expressed a lower level of c/EBPα, although this difference was not statistically significant (supplemental Fig. 3*A*). On the other hand, loss of CaMKK2 impaired accumulation of c/EBPβ and c/EBPδ mRNAs (Fig. 4*C*). These data are of particular interest due to the ability of c/EBP family members to extensively regulate the TLR-induced transcription program of macrophages (27, 28).

CaMKK2 Is Required for Macrophage Morphological Changes Induced by LPS—One of the earliest cellular responses to LPS in macrophages is cell spreading, a phenomenon largely induced by the β2-integrin family, which is mediated by a process called "inside-out" signaling (29). Macrophage spreading involves cytoskeletal reorganization as well as changes in integrin clustering and affinity for their cognate ligands. In the course of our investigation on the effects of CaMKK2, we found that BMDM macrophages generated from CaMKK2-null mice failed to acquire the typical morphology characteristically seen in response to LPS. To quantify this response, WT and CaMKK2$^{-/-}$ BMDM macrophages were grown on glass coverslips in the presence of 10% serum and then treated or not treated with LPS (100 ng/ml). After 24 h, macrophages were fixed, permeabilized, and stained with phalloidin to evaluate the morphological changes induced by LPS. Quiescent WT and CaMKK2$^{-/-}$ macrophages showed a similar elongated shape with a comparable cell surface area (Fig. 5*A*). However, within 18 h of LPS addition, the majority of WT macrophages changed their morphology from elongated to flat and spread, as seen by visualization of the cytoskeleton. This change was associated with a significant increase in cell surface area (Fig. 5*A*). Of note, loss of CaMKK2 clearly attenuated the increase in the macrophage surface area induced by LPS (Fig. 5*A*). The impairment of CaMKK2 KO macrophages to change morphology in response to LPS was also confirmed in macrophages isolated from peri-

toneal lavage of WT and CaMKK2 KO mice (supplemental Fig. 4). Because these data implied an altered ability of CaMKK2 macrophages to appropriately remodel the cytoskeleton in response to TLR4 stimulation, we explored their ability to phagocytose bacterial particles, a function regulated by TLR4 stimulation and requiring extensive cytoskeleton remodeling (30–32). To this end, we cultured WT and CaMKK2 KO BMDM for 24 h in the presence or absence of LPS and then examined their ability to phagocytose pH-rhodamine-conjugated *E. coli*. We found a remarkable decrease in the ability of quiescent CaMKK2 KO macrophages to phagocytose bacteria as compared with WT (Fig. 5*B*). The exposure of WT macrophages to increasing doses of LPS for 24 h induced a dose-dependent increase in their phagocytic activity. On the contrary, only a slight increase in ability to phagocytose bacteria was observed in LPS-stimulated CaMKK2 KO macrophages (Fig. 5*B*). Overall, these findings prompted us to hypothesize an important role for CaMKK2 in signaling pathways controlling cytoskeleton reorganization in response to TLR4 stimulation.

Loss of CaMKK2 Uncouples TLR4 Signaling from Activation of the Adhesion Kinase, PYK2—The engagement of TLR4 of agonist ligand triggers multiple signal cascades that include the activation of NFκB and MAPK (33). Stimulation of TLR4 also triggers the activation of PYK2, a major cell adhesion-activated kinase involved in mechanisms regulating spreading, migration, and cytokine synthesis in macrophages and other cell types (34–37). Because CaMKK2 KO macrophages showed an impaired ability to spread and phagocytose bacterial particles, we hypothesized an involvement of CaMKK2 in signals regulating accumulation of activated Tyr^{402}-phospho-PYK2 (pPYK2). Accordingly, we evaluated the levels of pPYK2 in WT and CaMKK2 KO macrophages cultured in the presence or absence of LPS. pPYK2 was detectable in quiescent WT macrophages and accumulated upon LPS stimulation as function of time (supplemental Fig. 5). Loss of CaMKK2 resulted in a slight decrease of pPYK2 in quiescent macrophages. Moreover, significantly less pPYK2 accumulated over time in CaMKK2 KO macrophages as compared with WT (40 and 50% of inhibition were detected at 15 and 120 min, respectively; supplemental Fig. 5). In macrophages and other cell types, PYK2 has been proposed to act as an amplifier for multiple signal cascades, and its loss has been found to be associated with decreased activation of NFκB, MAPKs, and AKT (34, 35, 38–41). Thus, we evaluated whether loss of CaMKK2 also affected these PYK2-regulated biochemical changes and found that CaMKK2 KO macrophages accumulated less phospho-p65 NFκB than WT in response to LPS (Fig. 6*A*, supplemental Fig. 5). Moreover, loss of CaMKK2 also impaired the ability of LPS-stimulated macrophages to accumulate the phosphorylated forms of ERK1/2, c-Jun, and AKT (Fig. 6*A*, supplemental Fig. 5). On the other hand, LPS-stimulated WT and CaMKK2 KO macrophages expressed comparable levels of phosho-p38 (Fig. 6*A*, supplemental Fig. 5). On the whole, these findings reveal an important role for CaMKK2 in the signal networks coupling the TLR4 cascade with activation of the cell adhesion kinase PYK2.

CaMKK2 Is Required for Attachment-dependent Amplification of TLR4 Signaling—It has been previously demonstrated that in human monocytes, adherence potentiates the secretion of TNFα induced by LPS through a mechanism that requires PYK2 activation and cytoskeleton reorganization (42, 43). Based on these findings, we hypothesized that loss of CaMKK2 impaired an adhesion-dependent amplifier circuit controlling PYK2 activation in response to TLR4 stimulation. To investigate this hypothesis, WT and CaMKK2 KO BMDM were adhered to regular cell culture plastic dishes, or kept in suspension for 1 h, before being exposed to increasing doses of LPS. As already shown in Fig. 4*A*, adherent WT BMDM secreted much larger amounts of TNFα as compared with CaMKK2-null macrophages (Fig. 6*B*). On the other hand, loss of adherence led to a marked impairment of LPS-induced TNFα secretion in WT but not $CaMKK2^{-/-}$ macrophages (Fig. 6*B*). Thus, we reasoned that loss of adherence would attenuate PYK2 activation and, in turn, TNFα secretion. Accordingly, we investigated PYK2/pPYK expression in adherent and nonadherent WT and CaMKK2 KO macrophages cultured in the presence or absence of LPS. We confirmed that genetic ablation of CaMKK2 impaired the ability of adherent macrophages to accumulate pPYK2 in response to LPS (Fig. 6, *C* and *D*). Of note, we also found that loss of CaMKK2 significantly decreased the level of total PYK2 (Fig. 6, *C* and *D*). In the absence of adhesion, pPYK2 was barely detectable in either WT or CaMKK2 KO cells (Fig. 6, *C* and *D*). Finally, WT and $CaMKK2^{-/-}$ macrophages kept in suspension expressed comparable lower levels of PYK2 (Fig. 6, *C* and *D*). To investigate the mechanisms underlying the decreased expression of PYK2, we measured PYK2 mRNA in quiescent and 1-h LPS-stimulated BMDM. Independent of genotype and culture conditions, BMDM expressed comparable levels of PYK2 mRNA (Fig. 6*D*, *lower right*).

The data described above suggested to us that CaMKK2-dependent signaling must regulate the expression of PYK2/pPYK2 by mechanisms not involving transcription or stability of PYK2 mRNA. One additional possibility is that CaMKK2 might regulate the stability of the PYK2 protein. To test this idea, we evaluated whether caspase, calpain or proteasome inhibitors such as Z-VAD-FMK, *N*-acetyl-Leu-Leu-Met, and MG132 could compensate for the loss of CaMKK2 by restoring PYK2 expression but found none to be effective (Fig. 6*E*). Because it is known that the expression of several cell surface receptors and signal transduction molecules can be controlled by the endolysosomal degradation pathway (44–46), we reasoned that CaMKK2 might regulate the traffic of endosome vesicles and, in turn, prevent PYK2 degradation at the endolysosomal level. To investigate this possibility, we exposed WT and $CaMKK2^{-/-}$ BMDM to ammonium chloride (NH_4Cl), a weak base used to inhibit the acidification of endosomes-lysosomes (47) and found this treatment effective in restoring PYK2 expression in CaMKK2-null macrophages (Fig. 6*E*). Based on these findings, we suggest that CaMKK2-dependent signaling may regulate the expression of pPYK2/PYK2 by controlling the rate of recycling and degradation of the protein in the endolysosomal compartment.

DISCUSSION

Obesity is associated with an extensive remodeling of metabolic tissues characterized by recruitment of immune cells and chronic low-grade inflammation of metabolic tissues (48). Pre-

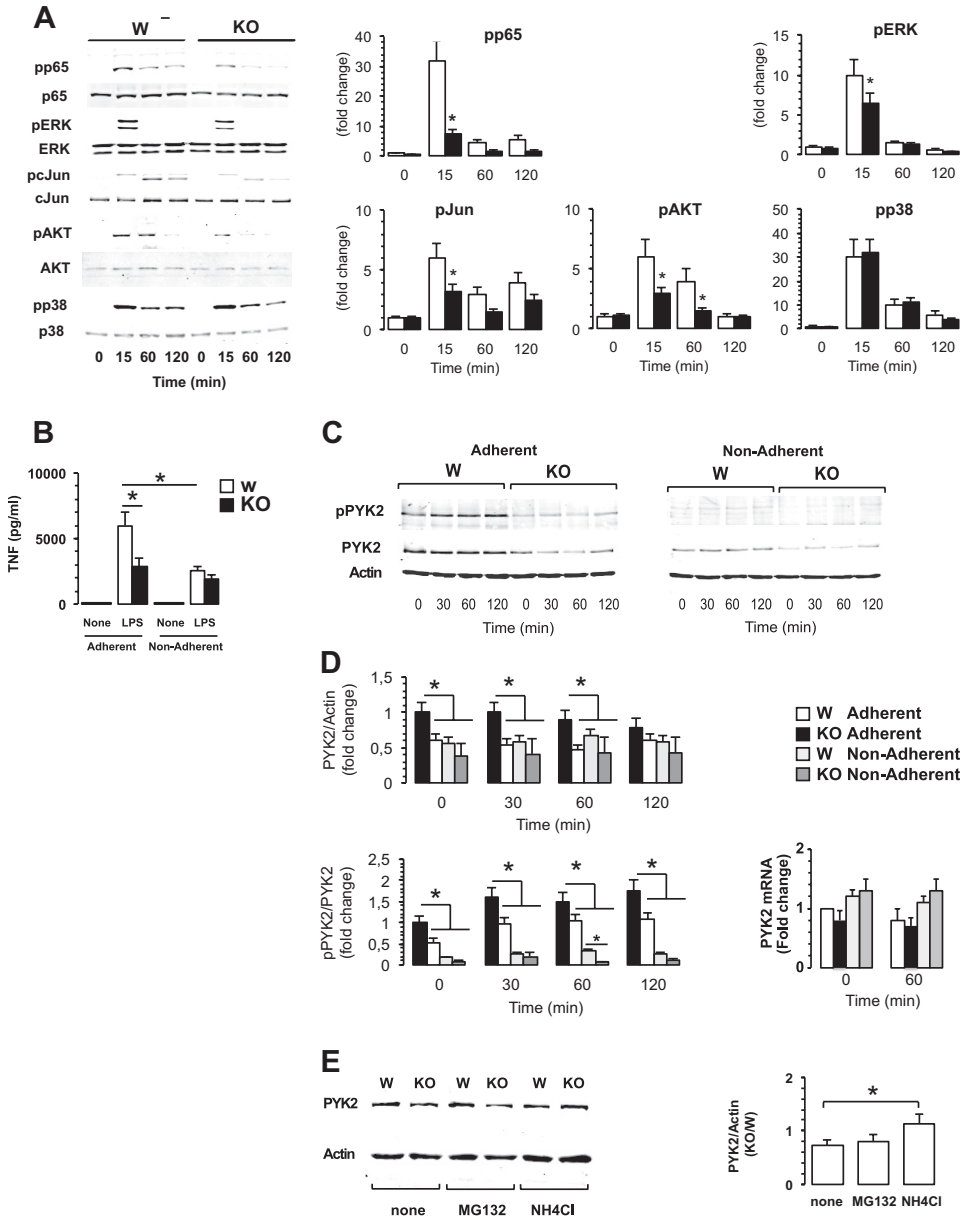

FIGURE 6. **Loss of CaMKK2 impairs TLR4-proximal signaling.** *A*, *left*, representative immunoblots from wild type (*W*) and CaMKK2$^{-/-}$ (*KO*) BMDM exposed to LPS (100 ng/ml). *Right*, graphs show quantitation of each specific phosphorylated band normalized to total and expressed as -fold change as compared with WT basal level. Means ± S.D. are calculated from five independent experiments (*open*, wild type; *black*, KO). *, $p < 0.001$. *pp65*, phospho-p65; *pERK*, phospho-ERK; *pcJun*, phospho-c-Jun; *pAKT*, phospho-AKT; *pp38*, phospho-p38. *B–D*, cell attachment regulation of macrophage responsiveness to LPS, demonstrating the role of CaMKK2. BMDM generated from WT and CaMKK2$^{-/-}$ mice (WT and KO, respectively) were adhered to plastic dishes or kept in suspension. After 2 h, cells were stimulated with LPS. *B*, TNFα concentration in 18-h supernatant fluids. *C*, representative immunoblots from WT and KO BMDM exposed for the indicated times to LPS (100 ng/ml). *D*, *upper* and *lower left*, graphs show quantitation of pPYK2 and PYK2 bands and are expressed as -fold change as compared with WT basal level. Means ± S.D. are calculated from four independent experiments (*open*, WT adherent; *black*, KO adherent; *light gray*, WT nonadherent; *dark gray*, KO adherent). *Lower right*, PYK2 mRNA detected at time 0 and 1-h LPS-stimulated WT and KO BMDM. *E*, representative immunoblots from WT and KO BMDM cultured for 2 h in the absence (*none*) or in the presence of the proteasome inhibitor MG132 (10 μM), or ammonium chloride (*NH4Cl*, 50 mM). *Right*, graphs show the relative PYK2/actin ratio expressed in CaMKK2 KO and WT macrophages. Means ± S.D. are calculated from three independent experiments. *, $p < 0.001$.

viously, we showed that CaMKK2 is an important component of ghrelin signaling in hypothalamic neurons, and its genetic ablation protects mice from HFD-induced obesity, insulin resistance, and glucose intolerance (13). Our findings herein that CaMKK2 deficiency dissociated obesity from inflammation and glucose intolerance led us to hypothesize a direct role for CaMKK2 in mechanisms regulating inflammation induced by overnutrition. We also found that CaMKK2 KO mice underwent an attenuated inflammatory response when exposed to bacterial endotoxin. Consequently, we investigated the expression of CaMKK2 in immune cells and found it to be restricted to cells of the monocytic/macrophage lineage. Indeed, in macrophages, the loss of CaMMK2 impaired important functions such as cytokine secretion, morphological changes, and phagocytosis. Mechanistically, we found that loss of CaMKK2 uncouples adhesion-dependent signals from the TLR4 cascade by interfering with accumulation of the phosphorylated forms of PYK2, ERK, Jun, AKT, and NFκB p65.

PYK2 is a member of the focal adhesion kinase (FAK) family and is highly expressed in the central nervous system and hematopoietic cells (49). Genetic ablation of PYK2 in macrophages interferes with multiple signaling events crucial for the appropriate morphology and migration of these cells. As examples, loss of PYK2 affects the ability of macrophages to become polarized, undergo membrane ruffling, and migrate in response to chemokine stimulation (35). The LPS-mediated accumulation of Tyr^{402}-pPYK2 has been reported by several authors, and this accumulation has been proposed to drive morphological changes and regulate the amplitude of TNFα release in response to LPS (34, 36, 37, 42). The role of PYK2 in the inflammatory response has also been demonstrated *in vivo* by showing that loss of PYK2, or its functional block, attenuated the infiltration of macrophages into a carrageenan-induced inflammatory region, as well as airway hyper-responsiveness in a mouse model of asthma (35, 50). Our findings that loss of CaMKK2 clearly affects the signal networks regulating the activation of PYK2, along with the remarkable similarities between the functional defects induced by genetic ablation of CaMKK2 and those observed in PYK2-null macrophages, reveal the CaMKK2/PYK2 pathway to be important in regulation of the molecular networks that govern the responsiveness of macrophages to external stimuli.

Several authors have proposed a role for CaMK family members in the regulation of macrophage and dendritic cell responsiveness to TLR4 agonists such as LPS. In these cell types, the activation of CaMK has been linked to either a TLR4-induced calcium transient or low, tonic, constitutive signals resulting from activation of other immune receptors (51–53). Single cell microfluorometric monitoring of calcium transients has provided direct evidence that LPS can trigger a heterogeneous response characterized by single rapid and transient, multiple transients, or most frequently, slower and more sustained increases in the intracellular calcium concentration (51). Furthermore, calcium measurements following administration of LPS to cells of the macrophage-like cell line RAW 264.7 have confirmed these changes in calcium concentration (53). On the other hand, a more recent study investigating the ability of a highly purified LPS preparation to trigger calcium transients in BMDM have raised doubts about this hypothesis (52). Thus, although a direct effect of TLR4 on the generation of calcium transients cannot be definitively ruled out, it has been established that tonic or low, constitutive calcium-dependent signaling sustained by integrins and other immune receptor tyrosine-based activation motif (ITAM)-coupled receptors plays an important role in fine-tuning the amplitude and nature of cellular responses to heterologous receptors such TLR4 (54–56). Moreover, by using such tonic signaling, myeloid cells could sense their environment and process this information to modulate responses to TLR and cytokine receptors (57). A seminal contribution to this hypothesis was generated from studies on the heterologous cross-regulation of INFα receptor by adhesion-coupled signals (55). In this study, pharmacological interrogation of cells with the calmodulin antagonist W-7, calcium chelator 1,2-bis(*o*-aminophenoxy)ethane-*N*,*N*,*N*′,*N*′-tetraacetic acid (BAPTA), and CaMK inhibitor KN93 led to the hypothesis that an ITAM receptor-coupled CaMK-dependent pathway controls PYK2 activation and, in turn, regulates the amplitude of the human monocyte responsiveness to INFα. However, no specific CaMK was discovered in this study. Here we show that an adhesion-dependent pathway links the TLR4 cascade with activation of PYK2 and tunes the amplitude of TNFα in LPS-stimulated macrophages. Notably, we define a specific CaMK, CaMKK2, to be an essential component of the adhesion-dependent heterologous signaling required for fine-tuning of TLR4-dependent signal cascade and the response of macrophages to an inflammatory stimulus.

Integrin ligation triggers a calcium-dependent pathway that promotes recruitment and autophosphorylation of PYK2 at the Tyr^{402} activating residue (58). This mechanism, however, only accounts for a partial activation of PYK2. The induction of full catalytic activity requires the binding of Src kinase via its SH2 domain to the autophosphorylated Tyr^{402} residue and the subsequent phosphorylation of PYK2 at functionally distinct sites, including Tyr^{579}, Tyr^{580}, and Tyr^{881} (59). However, the specific signaling network(s) involved in the regulation of PYK2 inactivation and degradation are less known. It has been demonstrated that Tyr^{402}-PYK2 can bind dynamin, a protein involved in the regulation of the endosome recycling pathway, and this event causes the efflux of Tyr^{402}-PYK2 from adhesion sites (60). Of interest, dynamin can also form a complex with syndapin I, a protein involved in regulation of vesicle recycling, which has been recently proposed as a novel substrate for CaMKK1 and CaMKK2 (61, 62). In addition to dynamin, the stability and subcellular localization of PYK2 can also be regulated by the E3-ubiquitin ligase Cbl, an enzyme that can form a complex with and regulate the proteasome-mediated degradation of PYK2 (63–65). Although the loss of integrin signaling may be sufficient to explain our finding that nonadherent LPS-stimulated WT macrophages fail to accumulate pPYK2 and secrete large amount of TNFα, it cannot explain the decrease of PYK2 phosphorylation that accompanies the loss of CaMKK2 because CaMKK2 is a serine/threonine kinase and therefore cannot directly activate PYK2 (59). However, we do find that the loss of CaMKK2 resulted in a substantial decrease of total PYK2, and this decrease in protein was not associated with a decrease of PYK2 mRNA. These data suggest the involvement of CaMKK2 in the mechanisms regulating stability and/or endosome recycling of pPYK2/PYK2. In this scenario, calcium signals from integrin (as well as from other ITAM-associated heterologous receptors) may sustain the tonic activation of CaMKK2. In turn, this could prevent the degradation of PYK2, thereby allowing this kinase to participate in other signal cascades such as that triggered by stimulation of TLR4. On the other hand, genetic ablation of CaMKK2, as well as the loss of integrin signaling, would limit PYK2 availability, block the heterologous cross-talk between integrin and other receptors involved in the regulation of the immune response, and prevent generation of the amplifier circuit coupling adhesion signals with the TLR4 cascade (see the model schematic in supplemental Fig. 6). Examination of this exciting possibility will fuel our future research efforts.

In conclusion, our findings uncover a novel and essential function for CaMKK2 in regulating the mechanisms that control the amplitude of the macrophage inflammatory response.

The restricted expression of CaMKK2 to a limited number of critical cell types makes this kinase an attractive target for therapies aimed at attenuating the detrimental effects of inflammation in metabolic disease and autoimmunity.

Acknowledgments—We thank Libby MacDougall for editing of the manuscript and Tom Ribar for technical assistance.

REFERENCES

1. Hook, S. S., and Means, A. R. (2001) Ca^{2+}/CaM-dependent kinases: from activation to function. *Annu. Rev. Pharmacol. Toxicol.* **41,** 471–505
2. Colomer, J., and Means, A. R. (2007) Physiological roles of the Ca^{2+}/CaM-dependent protein kinase cascade in health and disease. *Subcell. Biochem.* **45,** 169–214
3. Racioppi, L., and Means, A. R. (2008) Calcium/calmodulin-dependent kinase IV in immune and inflammatory responses: novel routes for an ancient traveler. *Trends Immunol.* **29,** 600–607
4. Liu, X., Zhan, Z., Xu, L., Ma, F., Li, D., Guo, Z., Li, N., and Cao, X. (2010) MicroRNA-148/152 impair innate response and antigen presentation of TLR-triggered dendritic cells by targeting CaMKIIα. *J. Immunol.* **185,** 7244–7251
5. Herrmann, T. L., Agrawal, R. S., Connolly, S. F., McCaffrey, R. L., Schlomann, J., and Kusner, D. J. (2007) MHC class II levels and intracellular localization in human dendritic cells are regulated by calmodulin kinase II. *J. Leukoc. Biol.* **82,** 686–699
6. Illario, M., Giardino-Torchia, M. L., Sankar, U., Ribar, T. J., Galgani, M., Vitiello, L., Masci, A. M., Bertani, F. R., Ciaglia, E., Astone, D., Maulucci, G., Cavallo, A., Vitale, M., Cimini, V., Pastore, L., Means, A. R., Rossi, G., and Racioppi, L. (2008) Calmodulin-dependent kinase IV links Toll-like receptor 4 signaling with survival pathway of activated dendritic cells. *Blood* **111,** 723–731
7. Nakaya, H. I., Wrammert, J., Lee, E. K., Racioppi, L., Marie-Kunze, S., Haining, W. N., Means, A. R., Kasturi, S. P., Khan, N., Li, G. M., McCausland, M., Kanchan, V., Kokko, K. E., Li, S., Elbein, R., Mehta, A. K., Aderem, A., Subbarao, K., Ahmed, R., and Pulendran, B. (2011) Systems biology of vaccination for seasonal influenza in humans. *Nat. Immunol.* **12,** 786–795
8. Zhang, X., Guo, L., Collage, R. D., Stripay, J. L., Tsung, A., Lee, J. S., and Rosengart, M. R. (2011) Calcium/calmodulin-dependent protein kinase (CaMK) Iα mediates the macrophage inflammatory response to sepsis. *J. Leukoc. Biol.* **90,** 249–261
9. Hurley, R. L., Anderson, K. A., Franzone, J. M., Kemp, B. E., Means, A. R., and Witters, L. A. (2005) The Ca^{2+}/calmodulin-dependent protein kinase kinases are AMP-activated protein kinase kinases. *J. Biol. Chem.* **280,** 29060–29066
10. Hawley, S. A., Pan, D. A., Mustard, K. J., Ross, L., Bain, J., Edelman, A. M., Frenguelli, B. G., and Hardie, D. G. (2005) Calmodulin-dependent protein kinase kinase-β is an alternative upstream kinase for AMP-activated protein kinase. *Cell Metab.* **2,** 9–19
11. Woods, A., Dickerson, K., Heath, R., Hong, S. P., Momcilovic, M., Johnstone, S. R., Carlson, M., and Carling, D. (2005) Ca^{2+}/calmodulin-dependent protein kinase kinase-β acts upstream of AMP-activated protein kinase in mammalian cells. *Cell Metab.* **2,** 21–33
12. Green, M. F., Anderson, K. A., and Means, A. R. (2011) Characterization of the CaMKKβ-AMPK signaling complex. *Cell. Signal.* **23,** 2005–2012
13. Anderson, K. A., Ribar, T. J., Lin, F., Noeldner, P. K., Green, M. F., Muehlbauer, M. J., Witters, L. A., Kemp, B. E., and Means, A. R. (2008) Hypothalamic CaMKK2 contributes to the regulation of energy balance. *Cell Metab.* **7,** 377–388
14. Lumeng, C. N., Maillard, I., and Saltiel, A. R. (2009) T-ing up inflammation in fat. *Nat. Med.* **15,** 846–847
15. Lehrke, M., and Lazar, M. A. (2004) Inflamed about obesity. *Nat. Med.* **10,** 126–127
16. Laskin, D. L., Sunil, V. R., Gardner, C. R., and Laskin, J. D. (2011) Macrophages and tissue injury: agents of defense or destruction? *Annu. Rev. Pharmacol. Toxicol.* **51,** 267–288
17. Olefsky, J. M., and Glass, C. K. (2010) Macrophages, inflammation, and insulin resistance. *Annu. Rev. Physiol.* **72,** 219–246
18. Stearns-Kurosawa, D. J., Osuchowski, M. F., Valentine, C., Kurosawa, S., and Remick, D. G. (2011) The pathogenesis of sepsis. *Annu. Rev. Pathol.* **6,** 19–48
19. Gutierrez-Ramos, J. C., and Bluethmann, H. (1997) Molecules and mechanisms operating in septic shock: lessons from knock-out mice. *Immunol. Today* **18,** 329–334
20. Gainetdinov, R. R., Bohn, L. M., Walker, J. K., Laporte, S. A., Macrae, A. D., Caron, M. G., Lefkowitz, R. J., and Premont, R. T. (1999) Muscarinic supersensitivity and impaired receptor desensitization in G protein-coupled receptor kinase 5-deficient mice. *Neuron* **24,** 1029–1036
21. Gong, S., Zheng, C., Doughty, M. L., Losos, K., Didkovsky, N., Schambra, U. B., Nowak, N. J., Joyner, A., Leblanc, G., Hatten, M. E., and Heintz, N. (2003) A gene expression atlas of the central nervous system based on bacterial artificial chromosomes. *Nature* **425,** 917–925
22. Ray, A., and Dittel, B. N. (2010) Isolation of mouse peritoneal cavity cells. *J. Vis. Exp.* **35,** e1488
23. Teng, E. C., Racioppi, L., and Means, A. R. (2011) A cell-intrinsic role for CaMKK2 in granulocyte lineage commitment and differentiation. *J. Leukoc. Biol.* **90,** 897–909
24. Bromley, S. K., Mempel, T. R., and Luster, A. D. (2008) Orchestrating the orchestrators: chemokines in control of T cell traffic. *Nat. Immunol.* **9,** 970–980
25. Locati, M., Otero, K., Schioppa, T., Signorelli, P., Perrier, P., Baviera, S., Sozzani, S., and Mantovani, A. (2002) The chemokine system: tuning and shaping by regulation of receptor expression and coupling in polarized responses. *Allergy* **57,** 972–982
26. Silva, M. T. (2010) When two is better than one: macrophages and neutrophils work in concert in innate immunity as complementary and cooperative partners of a myeloid phagocyte system. *J. Leukoc. Biol.* **87,** 93–106
27. Nerlov, C. (2010) Transcriptional and translational control of C/EBPs: the case for "deep" genetics to understand physiological function. *Bioessays* **32,** 680–686
28. Litvak, V., Ramsey, S. A., Rust, A. G., Zak, D. E., Kennedy, K. A., Lampano, A. E., Nykter, M., Shmulevich, I., and Aderem, A. (2009) Function of C/EBPδ in a regulatory circuit that discriminates between transient and persistent TLR4-induced signals. *Nat. Immunol.* **10,** 437–443
29. Abram, C. L., and Lowell, C. A. (2009) The ins and outs of leukocyte integrin signaling. *Annu. Rev. Immunol.* **27,** 339–362
30. Aderem, A., and Underhill, D. M. (1999) Mechanisms of phagocytosis in macrophages. *Annu. Rev. Immunol.* **17,** 593–623
31. Kong, L., Sun, L., Zhang, H., Liu, Q., Liu, Y., Qin, L., Shi, G., Hu, J. H., Xu, A., Sun, Y. P., Li, D., Shi, Y. F., Zang, J. W., Zhu, J., Chen, Z., Wang, Z. G., and Ge, B. X. (2009) An essential role for RIG-I in Toll-like receptor-stimulated phagocytosis. *Cell Host Microbe* **6,** 150–161
32. Blander, J. M., and Medzhitov, R. (2004) Regulation of phagosome maturation by signals from Toll-like receptors. *Science* **304,** 1014–1018
33. Ostuni, R., Zanoni, I., and Granucci, F. (2010) Deciphering the complexity of Toll-like receptor signaling. *Cell. Mol. Life Sci.* **67,** 4109–4134
34. Xi, C. X., Xiong, F., Zhou, Z., Mei, L., and Xiong, W. C. (2010) PYK2 interacts with MyD88 and regulates MyD88-mediated NFκB activation in macrophages. *J. Leukoc. Biol.* **87,** 415–423
35. Okigaki, M., Davis, C., Falasca, M., Harroch, S., Felsenfeld, D. P., Sheetz, M. P., and Schlessinger, J. (2003) Pyk2 regulates multiple signaling events crucial for macrophage morphology and migration. *Proc. Natl. Acad. Sci. U.S.A.* **100,** 10740–10745
36. Hazeki, K., Masuda, N., Funami, K., Sukenobu, N., Matsumoto, M., Akira, S., Takeda, K., Seya, T., and Hazeki, O. (2003) Toll-like receptor-mediated tyrosine phosphorylation of paxillin via MyD88-dependent and -independent pathways. *Eur. J. Immunol.* **33,** 740–747
37. Williams, L. M., and Ridley, A. J. (2000) Lipopolysaccharide induces actin reorganization and tyrosine phosphorylation of Pyk2 and paxillin in monocytes and macrophages. *J. Immunol.* **164,** 2028–2036
38. Avraham, H., Park, S. Y., Schinkmann, K., and Avraham, S. (2000) RAFTK/Pyk2-mediated cellular signaling. *Cell. Signal.* **12,** 123–133
39. Matsui, A., Okigaki, M., Amano, K., Adachi, Y., Jin, D., Takai, S., Yamashita, T., Kawashima, S., Kurihara, T., Miyazaki, M., Tateishi, K., Matsunaga, S., Katsume, A., Honshou, S., Takahashi, T., Matoba, S., Kusaba,

T., Tatsumi, T., and Matsubara, H. (2007) Central role of calcium-dependent tyrosine kinase PYK2 in endothelial nitric oxide synthase-mediated angiogenic response and vascular function. *Circulation* **116,** 1041–1051
40. Kelly, E. K., Wang, L., and Ivashkiv, L. B. (2010) Calcium-activated pathways and oxidative burst mediate zymosan-induced signaling and IL10 production in human macrophages. *J. Immunol.* **184,** 5545–5552
41. Iiizumi, M., Bandyopadhyay, S., Pai, S. K., Watabe, M., Hirota, S., Hosobe, S., Tsukada, T., Miura, K., Saito, K., Furuta, E., Liu, W., Xing, F., Okuda, H., Kobayashi, A., and Watabe, K. (2008) RhoC promotes metastasis via activation of the Pyk2 pathway in prostate cancer. *Cancer Res.* **68,** 7613–7620
42. Rosengart, M. R., Arbabi, S., Bauer, G. J., Garcia, I., Jelacic, S., and Maier, R. V. (2002) The actin cytoskeleton: an essential component for enhanced TNFα production by adherent monocytes. *Shock* **17,** 109–113
43. Rosengart, M. R., Arbabi, S., Garcia, I., and Maier, R. V. (2000) Interactions of calcium/calmodulin-dependent protein kinases (CaMK) and extracellular-regulated kinase (ERK) in monocyte adherence and TNFα production. *Shock* **13,** 183–189
44. Ye, S., Cihil, K., Stolz, D. B., Pilewski, J. M., Stanton, B. A., and Swiatecka-Urban, A. (2010) c-Cbl facilitates endocytosis and lysosomal degradation of cystic fibrosis transmembrane conductance regulator in human airway epithelial cells. *J. Biol. Chem.* **285,** 27008–27018
45. Baldys, A., and Raymond, J. R. (2009) Critical role of ESCRT machinery in EGFR recycling. *Biochemistry* **48,** 9321–9323
46. Wang, H., Holst, J., Woo, S. R., Guy, C., Bettini, M., Wang, Y., Shafer, A., Naramura, M., Mingueneau, M., Dragone, L. L., Hayes, S. M., Malissen, B., Band, H., and Vignali, D. A. (2010) Tonic ubiquitylation controls T cell receptor:CD3 complex expression during T cell development. *EMBO J.* **29,** 1285–1298
47. Gordon, A. H., Hart, P. D., and Young, M. R. (1980) Ammonia inhibits phagosome-lysosome fusion in macrophages. *Nature* **286,** 79–80
48. Gregor, M. F., and Hotamisligil, G. S. (2011) Inflammatory mechanisms in obesity. *Annu. Rev. Immunol.* **29,** 415–445
49. Schaller, M. D. (2010) Cellular functions of FAK kinases: insight into molecular mechanisms and novel functions. *J. Cell Sci.* **123,** 1007–1013
50. Duan, Y., Learoyd, J., Meliton, A. Y., Clay, B. S., Leff, A. R., and Zhu, X. (2010) Inhibition of Pyk2 blocks airway inflammation and hyper-responsiveness in a mouse model of asthma. *Am. J. Respir. Cell Mol. Biol.* **42,** 491–497
51. Letari, O., Nicosia, S., Chiavaroli, C., Vacher, P., and Schlegel, W. (1991) Activation by bacterial lipopolysaccharide causes changes in the cytosolic free calcium concentration in single peritoneal macrophages. *J. Immunol.* **147,** 980–983
52. Zanoni, I., Ostuni, R., Capuano, G., Collini, M., Caccia, M., Ronchi, A. E., Rocchetti, M., Mingozzi, F., Foti, M., Chirico, G., Costa, B., Zaza, A., Ricciardi-Castagnoli, P., and Granucci, F. (2009) CD14 regulates the dendritic cell life cycle after LPS exposure through NFAT activation. *Nature* **460,** 264–268
53. Liu, X., Yao, M., Li, N., Wang, C., Zheng, Y., and Cao, X. (2008) CaMKII promotes TLR-triggered proinflammatory cytokine and type I interferon production by directly binding and activating TAK1 and IRF3 in macrophages. *Blood* **112,** 4961–4970
54. Ivashkiv, L. B. (2009) Cross-regulation of signaling by ITAM-associated receptors. *Nat. Immunol.* **10,** 340–347
55. Wang, L., Tassiulas, I., Park-Min, K. H., Reid, A. C., Gil-Henn, H., Schlessinger, J., Baron, R., Zhang, J. J., and Ivashkiv, L. B. (2008) "Tuning" of type I interferon-induced Jak-STAT1 signaling by calcium-dependent kinases in macrophages. *Nat. Immunol.* **9,** 186–193
56. Turnbull, I. R., and Colonna, M. (2007) Activating and inhibitory functions of DAP12. *Nat. Rev. Immunol.* **7,** 155–161
57. Klesney-Tait, J., Turnbull, I. R., and Colonna, M. (2006) The TREM receptor family and signal integration. *Nat. Immunol.* **7,** 1266–1273
58. Duong, L. T., and Rodan, G. A. (2000) PYK2 is an adhesion kinase in macrophages, localized in podosomes and activated by β_2-integrin ligation. *Cell Motil. Cytoskeleton* **47,** 174–188
59. Lowell, C. A. (2011) Src family and Syk kinases in activating and inhibitory pathways in innate immune cells: signaling cross talk. *Cold Spring Harb. Perspect. Biol.* **3,** a002352
60. Bruzzaniti, A., Neff, L., Sandoval, A., Du, L., Horne, W. C., and Baron, R. (2009) Dynamin reduces Pyk2 Tyr^{402} phosphorylation and SRC binding in osteoclasts. *Mol. Cell. Biol.* **29,** 3644–3656
61. Fujimoto, T., Hatano, N., Nozaki, N., Yurimoto, S., Kobayashi, R., and Tokumitsu, H. (2011) Identification of a novel CaMKK substrate. *Biochem. Biophys. Res. Commun.* **410,** 45–51
62. Anggono, V., Smillie, K. J., Graham, M. E., Valova, V. A., Cousin, M. A., and Robinson, P. J. (2006) Syndapin I is the phosphorylation-regulated dynamin I partner in synaptic vesicle endocytosis. *Nat. Neurosci.* **9,** 752–760
63. Sanjay, A., Houghton, A., Neff, L., DiDomenico, E., Bardelay, C., Antoine, E., Levy, J., Gailit, J., Bowtell, D., Horne, W. C., and Baron, R. (2001) Cbl associates with Pyk2 and Src to regulate Src kinase activity, $\alpha_v\beta_3$ integrin-mediated signaling, cell adhesion, and osteoclast motility. *J. Cell Biol.* **152,** 181–195
64. Haglund, K., Ivankovic-Dikic, I., Shimokawa, N., Kruh, G. D., and Dikic, I. (2004) Recruitment of Pyk2 and Cbl to lipid rafts mediates signals important for actin reorganization in growing neurites. *J. Cell Sci.* **117,** 2557–2568
65. Sekine, Y., Tsuji, S., Ikeda, O., Sugiyma, K., Oritani, K., Shimoda, K., Muromoto, R., Ohbayashi, N., Yoshimura, A., and Matsuda, T. (2007) Signal-transducing adaptor protein-2 regulates integrin-mediated T cell adhesion through protein degradation of focal adhesion kinase. *J. Immunol.* **179,** 2397–2407